



# Production of neutrinos and secondary electrons in cosmic sources

C.-Y. Huang\*, M. Pohl

*Department of Physics and Astronomy, Iowa State University, Ames, IA 50011, United States*

Received 15 November 2007; received in revised form 23 January 2008; accepted 9 February 2008

## Abstract

We study the individual contribution to secondary lepton production in hadronic interactions of cosmic rays (CRs) including resonances and heavier secondaries. For this purpose we use the same methodology discussed earlier [C.-Y. Huang, S.-E. Park, M. Pohl, C.D. Daniels, *Astropart. Phys.* 27 (2007) 429], namely the Monte-Carlo particle collision code DPMJET3.04 to determine the multiplicity spectra of various secondary particles with leptons as the final decay states, that result from inelastic collisions of cosmic-ray protons and Helium nuclei with the interstellar medium of standard composition. By combining the simulation results with parametric models for secondary particle (with resonances included) for incident cosmic-ray energies below a few GeV, where DPMJET appears unreliable, we thus derive production matrices for all stable secondary particles in cosmic-ray interactions with energies up to about 10 PeV.

We apply the production matrices to calculate the radio synchrotron radiation of secondary electrons in a young shell-type SNR, RX J1713.7-3946, which is a measure of the age, the spectral index of hadronic cosmic rays, and most importantly the magnetic field strength. We find that the multi-mG fields recently invoked to explain the X-ray flux variations are unlikely to extend over a large fraction of the radio-emitting region, otherwise the spectrum of hadronic cosmic rays in the energy window 0.1–100 GeV must be unusually hard.

We also use the production matrices to calculate the muon event rate in an IceCube-like detector that are induced by muon neutrinos from high-energy  $\gamma$ -ray sources such as RX J1713.7-3946, Vela Jr. and MGRO J2019+37. At muon energies of a few TeV, or in other word, about 10 TeV neutrino energy, an accumulation of data over about 5–10 years would allow testing the hadronic origin of TeV  $\gamma$ -rays.

© 2008 Published by Elsevier B.V.

*PACS:* 13.85.Tp; 95.85.Ry; 98.70.Sa; 98.38.Mz

*Keywords:* Cosmic rays; Cosmic-ray interactions; Neutrino and lepton astronomy; Supernova remnants

## 1. Introduction

It is known that hadronic cosmic rays interacting with the interstellar medium (ISM) can produce  $\gamma$ -rays and leptons. The principal production mechanisms for  $\gamma$ -rays in high-energy astrophysics are inelastic CR+ISM interactions with subsequent decays of the secondaries (mostly the neutral  $\pi^0$  and  $\eta$ ) into  $\gamma$ -rays. The decays of charged  $\pi^\pm$  mesons and other secondaries will result in the production of high-energy neutrinos and secondary leptons, elec-

trons and positrons. In GeV-scale Galactic cosmic rays, the secondary electrons and positrons comprise around 20% of the total electron flux and significantly contribute to the non-thermal electromagnetic radiation of  $\gamma$ -ray sources. The flux of cosmic-ray neutrinos is determined by the cosmic-ray abundance and the production cross sections of the parent particles ( $\pi^\pm$ ,  $K^\pm$ ,  $K_S^0$ ,  $K_L^0$ ,  $\Sigma^\pm$ ,  $\Sigma^0$ ,  $\Lambda$ ,  $\bar{\Lambda}$ ) in the collisions of cosmic rays with the interstellar gas nuclei.

The purpose of this work is to carefully calculate the lepton production in cosmic-ray interactions. For this purpose we use the high-energy physics event generator DPMJET-III [2] to simulate all secondary productions in both p-generated and He-generated interactions, similar to earlier work on hadronic  $\gamma$ -ray production [1]. Our study includes

\* Corresponding author. Tel.: +1 515 2945062; fax: +1 515 2946027.  
E-mail address: huangc@iastate.edu (C.-Y. Huang).

direct lepton production and the decays of all relevant secondary particles with leptons as the final decay products. For the cosmic rays, protons and helium nuclei are taken into account. We assume the composition of the ISM as 90% protons, 10% helium nuclei, 0.02% carbon, and 0.04% oxygen. At energies below 20 GeV, where DPMJET appears unreliable, we combine the simulation results with parametric models for  $\pi^\pm$  and  $\pi^0$  production [3,4] that include the production of the resonances  $\Delta(1232)$  and  $\Delta(1600)$  and their subsequent decays, thus deriving a lepton production matrix for cosmic rays with energies up to about 10 PeV that can be easily used to interpret the spectra of cosmic lepton sources.

We use our production matrices to calculate the CR-induced electron/positron production in young shell-type supernova remnants (SNR), for which the neutrino fluxes are also calculated. Observations of non-thermal X-ray synchrotron radiation from the SNRs SN 1006 [5], RX J1713.7-3946 [6], IC 443 [7,8], Cas A [9], and RCW 86 [10] support the hypothesis that the Galactic cosmic-ray electrons may be accelerated predominantly in SNR, although other acceleration sites of high-energy electrons might exist in the Galaxy. The existence of electrons in SNRs with an energy up to about 100 TeV implies TeV-scale  $\gamma$ -ray emission [11] besides that possibly produced by hadronic cosmic rays, and TeV-scale gamma-rays have indeed been detected from the SNRs Vela Junior [12] and RX J1713.7-3946 [13]. Although the hadronic interpretation is often favored to explain the  $\gamma$ -ray emission from SNRs such as RX J1713.7-3946 [13], there is still no direct observational evidence for nucleon acceleration in SNRs [14,1]. Currently, both hadronic and leptonic models can describe the observed TeV  $\gamma$ -rays in different astrophysical objects, but have problems of similar magnitude [15].

RX J1713.7-3946 is a unique SNR in the sense that its X-ray emission is strongly dominated by a non-thermal component, which is presumed to be synchrotron radiation of ultrarelativistic electrons (see Refs. [16–18] and references therein for details). The recent broadband X-ray spectroscopy performed with Chandra [18] and the Suzaku experiment [19] provides evidence of very effective acceleration of particles in the shell of RX J1713.7-3946 and also reveals that the X-ray emission from two compact regions is variable in flux, which the authors interpret as indication of multi-mG magnetic fields. If this conclusion is correct and applies to the entire remnant, then the observed TeV-band  $\gamma$ -ray emission must be of hadronic origin. Here we show that the synchrotron flux from the secondary electrons in RX J1713.7-3946 would in fact exceed the observed radio flux from this object, if multi-mG magnetic fields would permeate the remnant, so a magnetic field of such magnitude will likely exist at most in a small fraction of emission region.

In a hadron accelerator, TeV neutrinos should be produced in roughly the same number as TeV  $\gamma$ -rays. The Universe is generally more transparent for high-energy neutrinos than for TeV and PeV  $\gamma$ -rays, that can be absorbed by pair production with either the microwave

background (CMB) or the infrared/optical photon background (IRB). Therefore the detection of astrophysical neutrinos can provide invaluable complementary information on the existence of hadronic processes at astrophysical objects. Here we calculate the observable TeV-scale neutrino flux from RX J1713.7-3946 and other sources. This is not the first attempt to do such work. In fact, several calculations of the expected  $\gamma$ -ray and neutrino spectra were made for parametrized hadronic particles in the energy range of neutrino detectors [20–26]. In contrast to the earlier works, we include all relevant channels of neutrino production and also we do not rely on assuming a simple power-law proton spectrum or a power-law with an exponential cut-off, because our neutrino production matrix can be applied to energetic particles with arbitrary spectrum.

## 2. Inelastic cosmic-ray interactions

### 2.1. Set-up of the Monte-Carlo event generator DPMJET-III

This work uses the same method to determine the  $\gamma$ -ray production matrix for the cosmic-ray hadronic interactions as published earlier for  $\gamma$ -ray production [1], namely applying the Monte-Carlo event generator, DPMJET-III [2], to simulate the secondary production in cosmic-ray interactions. The readers are referred to Ref. [1] for the details of this technique.

### 2.2. Decay channels of secondary particles to leptons

All secondary particles produced in simulated hadronic interactions are recorded while running the event generator DPMJET-III. The following decay modes show all the decay processes of secondary products with leptons as the final decay particles, that are taken into account. Stable leptons considered in this work are  $e^\pm$ ,  $\nu_e$ ,  $\bar{\nu}_e$ ,  $\nu_\mu$ , and  $\bar{\nu}_\mu$ . Note that the lifetime of neutrons is about 886 s, much shorter than the propagation time scale of cosmic-ray particles in the Galaxy. Therefore, the neutrons are treated as having decayed entirely in this work. The decay channels considered in this work are as follows.

- baryonic decays:

$$n \rightarrow p + e^- + \bar{\nu}_e,$$

$$\bar{n} \rightarrow \bar{p} + e^+ + \nu_e,$$

$$\Lambda \rightarrow \begin{cases} p + \pi^-, \\ n + \pi^0, \end{cases}$$

$$\bar{\Lambda} \rightarrow \begin{cases} \bar{p} + \pi^+, \\ \bar{n} + \pi^0, \end{cases}$$

$$\Sigma^0 \rightarrow \Lambda + \gamma,$$

$$\Sigma^+ \rightarrow \begin{cases} p + \pi^0, \\ n + \pi^+, \end{cases}$$

$$\Sigma^- \rightarrow n + \pi^-.$$

149

150

- mesonic decays:

$$\pi^+ \rightarrow \mu^+ + \nu_\mu,$$

$$\pi^- \rightarrow \mu^- + \bar{\nu}_\mu,$$

$$\pi^0 \rightarrow e^+ + e^- + \gamma,$$

$$K^+ \rightarrow \begin{cases} \mu^+ + \nu_\mu, \\ \pi^+ + \pi^0, \end{cases}$$

$$K^- \rightarrow \begin{cases} \mu^- + \bar{\nu}_\mu, \\ \pi^- + \pi^0, \end{cases}$$

$$K_S^0 \rightarrow \begin{cases} 2\pi^0, \\ \pi^- + \pi^+, \end{cases}$$

$$K_L^0 \rightarrow \begin{cases} 3\pi^0, \\ \pi^- + \pi^+ + \pi^0, \\ \pi^+ + e^- + \bar{\nu}_e, \\ \pi^- + e^+ + \nu_e, \\ \pi^+ + \mu^- + \bar{\nu}_\mu, \\ \pi^- + \mu^+ + \nu_\mu. \end{cases}$$

152

154

153

- leptonic decays:

$$\mu^+ \rightarrow e^+ + \nu_e + \bar{\nu}_\mu,$$

$$\mu^- \rightarrow e^- + \bar{\nu}_e + \nu_\mu,$$

$$\tau^+ \rightarrow \begin{cases} \mu^+ + \nu_\mu + \bar{\nu}_\tau, \\ e^+ + \nu_e + \bar{\nu}_\tau, \end{cases}$$

$$\tau^- \rightarrow \begin{cases} \mu^- + \bar{\nu}_\mu + \nu_\tau, \\ e^- + \bar{\nu}_e + \nu_\tau. \end{cases}$$

157

158

159

160

161

162

163

164

165

166

167

168

In the DPMJET simulation setup, the decay of  $\eta$  mesons produced in the hadronic interactions has already been treated in the simulation. In our study on cosmic-ray-induced  $\gamma$ -ray production [1], we have verified that the  $\eta$  mesons are properly accounted for by performing test runs under different PYTHIA parameters, for which the  $\eta$  decays can be avoided in the simulation. We have also performed another independent verification using the very small contribution to  $e^-/e^+$  and  $\mu^-/\mu^+$  pairs from  $\eta$  decays, which are found consistent within the statistical uncertainty with all  $\eta$  mesons having decayed.

169

170

171

172

173

174

175

176

177

178

179

180

181

The  $\pi^\pm$  decays and subsequent  $\mu^\pm$  decays via the  $\pi - \mu - e$  decay chain are dominant in cosmic-ray interactions because pions carry the highest multiplicity among all the secondaries. We ignore neutrino production by charmed particles such as  $D$  and  $\bar{D}$ , because they contribute only at  $E_\nu \gtrsim 100$  TeV [27], where they are ignorable compared with neutrino production by pions. In the case of decays of moving  $\pi^\pm$ 's, the  $\pi$  energy is roughly equally divided among the four decay products, and thus the flux ratios are approximately  $(\nu_e, +\bar{\nu}_e)/(\nu_\mu + \bar{\nu}_\mu) = 1/2$  and  $\bar{\nu}_\mu/\nu_\mu = 1$ , no matter what the  $\pi$  spectrum is. In reality, however, these neutrino ratios may vary on account of the decays of heavier baryons and mesons. An excess of  $\mu^+$  mul-

tiplicity arises because more  $\pi^+$ 's than  $\pi^-$ 's are produced, and so the ratios  $\nu_e/\bar{\nu}_e$  and  $\bar{\nu}_\mu/\nu_\mu$  are somewhat increased.

For the two-body decay processes, the decay spectra are evaluated by particle kinematics; for the electrons/positrons from muon decays, the decay spectra are calculated by Lorentz transformation of the particle distribution in the center-of-mass system of the muon [28], which also includes the effect of the  $\mu$  polarization [29,30]; for kaon decays and heavy nucleon decays, the Dalitz-plot distribution is applied. The values published in Particle Data Group are employed for the fraction of each individual decay process.

### 2.3. Resonance contribution at low energies

In our earlier work on  $\gamma$ -ray production [1] we already found that DPMJET is unreliable below a few GeV collision energy. At these energies we therefore use a parametric model [4] to calculate the resultant decay spectra of  $\gamma$ ,  $e^\pm$ ,  $\nu_e(\bar{\nu}_e)$  and  $\nu_\mu(\bar{\nu}_\mu)$ . For the decay of the resonances  $\Delta(1232)$  and  $\Delta(1600)$  we assume the pion momentum to be isotropically distributed in the center-of-mass system and no angular correlation between the two pions in  $\Delta(1600)$  decay.

Note that the parametric model for pion and resonance production at low incident energies is for pp interactions only. We then use DPMJET to calculate the energy-dependent weight factors, which allow us to parametrically account for p + ISM and He + ISM collisions in the parametrization approach, even though it is derived for pp collisions only. The weight factors carry no strong dependence on the energy of the projectile particle.

### 3. The production matrix of secondary leptons generated by cosmic rays

The differential production rate of a final secondary particle is given by

$$Q_{2nd}(E) = \frac{dn}{dt \cdot dE \cdot dV} = n_{ISM} \int_{E_{CR}} dE_{CR} N_{CR}(E_{CR}) c \beta_{CR} \left( \sigma \frac{dn}{dE} \right), \quad (1)$$

with  $N_{CR}(E_{CR}) = \frac{dn_{CR}}{dE_{CR} dV} (\text{GeV cm}^3)^{-1}$  as the differential density of CR particles (p or  $\alpha$ ).

The differential cross section of a secondary particle produced in (p,  $\alpha$ )-ISM collisions is

$$\frac{d\sigma}{dE}(E_{CR}, E) = \sigma_{prod} \frac{dn}{dE}, \quad (2)$$

where  $\sigma_{prod}$  is the inelastic production cross section, i.e., the sum of diffraction, non-diffraction and resonance components whose values are calculated by DPMJET and the parametric model;  $\frac{dn}{dE}$  is the multiplicity spectrum of the secondary particle in question.

We follow the decay of unstable secondary particles to stable particles, and thus obtain the final spectrum of the stable secondaries  $\gamma$ -rays,  $e^\pm$ ,  $\nu_e$ ,  $\bar{\nu}_e$ ,  $\nu_\mu$  and  $\bar{\nu}_\mu$  as

$$Q_{2\text{nd}}(E_i) = \sum_k n_{\text{ISM}} \int_{E_{\text{CR}}} dE_{\text{CR}} N_{\text{CR}}(E_{\text{CR}}) c \beta_{\text{CR}} \sigma(E_{\text{CR}}) \times \frac{dn_{k,i}}{dE_i}(E_i, E_{\text{CR}}), \quad (3)$$

where  $\frac{dn_{k,i}}{dE_i}$  is the multiplicity spectrum of stable particle species  $i$  resulting from production channel  $k$ , either an unstable secondary or direct production. For binned particle spectra the production integral, Eq. (3), can be re-written as

$$Q_{2\text{nd}}(E_i) = n_{\text{ISM}} \sum_j \Delta E_j N_{\text{CR}}(E_j) c \beta_j \sigma(E_j) \sum_k \frac{dn_{k,i}}{dE_i}(E_i, E_j) = n_{\text{ISM}} \sum_j \Delta E_j N_{\text{CR}}(E_j) c \beta_j \sigma_j \mathbb{M}_{ij} \quad (4)$$

for the secondary particle of interest. In Eqs. (4) and (5), the energies for cosmic-ray particles ( $p$  or  $\alpha$ ) and the secondary particles are parametrized as [1]:

$$E_T = 1.24 \cdot (1 + 0.05)^j \text{ GeV/n} \quad \text{for cosmic rays,} \quad (6)$$

$$E_k = 0.01 \cdot (1.121376)^{i-0.5} \text{ GeV} \quad \text{for secondary particles,} \quad (7)$$

$n_{\text{ISM}} \simeq 1.11 n_H$  in Eq. (5) accounts for the specific element abundance in the ISM assumed 90% H, 10% He, 0.04% O and 0.02% C here. Please note that the ratio of the  $\gamma$ -ray and neutrino yields is independent of  $n_{\text{ISM}}$ . The main product of our work is the production matrix  $\mathbb{M}_{ij}$  that describes the production spectrum of the stable secondary particles, one for each, for arbitrary cosmic-ray spectra, separately for protons and Helium nuclei.

#### 4. Applications: SNR

With the production matrix established for each stable particle, we are now in the position to calculate the production spectra of secondary leptons and neutrinos in a variety of sources. As an example we here consider young shell-type SNRs. Being associated with dense gas along the line-of-sight, the shell-type SNR RX J1713.7-3946 could provide significant information on the acceleration of hadronic cosmic rays. In addition, RX J1713.7-3946 is also a unique supernova remnant in the sense that its X-ray emission is strongly dominated by a non-thermal component, which is presumed to be synchrotron radiation of ultrarelativistic electrons. These electrons also produce TeV-band gamma-rays, but would require a relatively small magnetic field to account for the TeV-band  $\gamma$ -ray spectrum observed with HESS [13]. The recently observed rapid variability of X-rays of RX J1713.7-3946 has been interpreted as evidence of a multi-mG magnetic field [18], in which case the leptonic scenario would be untenable.

We can test this interpretation by calculating the synchrotron radiation of secondary electrons in this remnant. In an earlier paper we have determined the cosmic-ray

spectrum in RX J1713.7-3946 under the assumption that the observed TeV-band spectrum is hadronic in origin [1]. Using our newly derived production matrix for secondary electrons and positrons, we can determine the differential production rate of those particles which, together with a time-dependent cosmic-ray continuity equation, allows us to calculate the radio synchrotron radiation of the secondary electrons with mainly the magnetic field strength as a fully free parameter.

Our fit of the TeV  $\gamma$ -ray spectrum constrains only the strongly curved cosmic-ray spectrum in the 1–100 TeV energy range. However, synchrotron emission in the GHz range is produced by GeV-scale electrons and we do not know how the spectrum continues down to GeV energies. So for simplicity, we match a single-power-law spectrum to the multi-TeV spectrum of cosmic-ray nucleons that we derive from fitting the HESS data,

$$N(E) = N_0 \left( \frac{E}{E_0} \right)^{-s+\sigma \ln \frac{E}{E_0}} \exp \left( -\frac{E}{E_{\text{max}}} \right), \quad E \geq E_c, \quad (8)$$

$$N(E) = M_0 \left( \frac{E}{E_0} \right)^{-\alpha}, \quad E < E_c, \quad (9)$$

where the parameters in Eq. (8) are derived by fitting the observed TeV-band  $\gamma$ -ray spectrum of RX J1713.7-3946 [1,31]. In this parametrization,  $E_0 = 15$  TeV is a normalization chosen to render uncorrelated the variations in the power-law index,  $s$ , and the spectral curvature,  $\sigma$ .  $E_{\text{max}}$  is the cut-off energy, and the best-fitting parameter values are  $s = 2.13$ ,  $\sigma = -0.25$ , and  $E_{\text{max}} \gtrsim 200$  TeV.  $N_0$  is the overall normalization, determined by the integral spectrum of  $\gamma$ -rays above 1 TeV [13]. If a numerical value of  $\alpha$  is set, the normalization  $M_0$  and the merging energy  $E_c$  are fully determined by the two continuity conditions that link the two spectral forms (8) and (9). Models of particle acceleration in cosmic-ray modified shocks suggest that the spectral index  $\alpha$  should be slightly smaller than 2 [32,33]. Note that  $\alpha$  denotes the average particle spectral index between about 1 GeV and 10 TeV. The combined cosmic-ray spectrum together with our production matrices for electrons and positrons then yields the differential production rate of secondary leptons that is implied by the  $\gamma$ -ray spectrum observed from RX J1713.7-3946.

##### 4.1. Electrons/positrons

Secondary electrons have been accumulated in the remnant since it commenced hadron acceleration. To determine the synchrotron radiation of the secondary electrons, we must obtain the electron spectrum in the SNR by solving a simplified time-dependent electron transport equation:

$$\frac{\partial N}{\partial t} + \frac{\partial}{\partial E} (b(E)N) = Q(E, T), \quad (10)$$

where  $T$  is the time after supernova explosion and the electron energy loss rate is that for synchrotron radiation

$$b(E) = \dot{E} = -\frac{4}{3}\sigma_{\text{Th}}cU_B\beta^2\gamma^2 = -\frac{4}{3}\sigma_{\text{Th}}c\frac{B^2}{2\mu_0}\beta^2\gamma^2, \quad (11)$$

with  $U_B$  as the energy density of the magnetic field and  $\sigma_{\text{Th}}$  as the Thomson cross section.

The likely distance to RX J1713.7-3946 is 1 kpc and the implied age would be about 1600 years [6,18,34]. An alternative kinematic solution places the remnant at about 6 kpc in distance with implied age of 10,000 years [8]. Whatever the acceleration history of the remnant is, cosmic-ray particles which have been accelerated early in its evolution will have lost some of their energy by adiabatic expansion, with most of it happening very early in the evolution. To be conservative we therefore consider only half of the remnant age, during which we assume the differential production rate of secondary electrons,  $q(E)$ , to be constant and given by our production matrix and the cosmic-ray spectrum as in Eqs. (8) and (9)

$$Q(E, T) = q(E)\Theta(T - t_{1/2}). \quad (12)$$

Then the spectrum of secondary electrons or positrons is obtained by integrating the Green function and the source term over time and energy:

$$N(E, T) = \int \int dE_0 dT_0 q(E_0)\Theta(T_0 - t_{1/2}) \times \frac{\delta(T - T_0 - \tau)}{|b(E)|} \Theta(E_0 - E), \quad (13)$$

where  $\tau = \int_{E_0}^E \frac{dE'}{b(E')}$  is the electron cooling time. For high energies  $\tau \leq t_{1/2}$  and the spectrum is loss-limited, i.e. essentially steepened by 1 in the spectral index, whereas at low energies the production spectrum is preserved. Note that the synchrotron flux calculated using the electron spectrum (13) is absolutely normalized by the TeV  $\gamma$ -ray flux.

Fig. 1 shows an example of the synchrotron spectrum from RX J1713.7-3946 that is contributed by secondary electrons assuming a distance of 1 kpc, the age as 1600 years, and the power-law index  $\alpha = 1.8$  for the multi-GeV cosmic-ray nucleon spectrum. The synchrotron spectra for three different values of the magnetic fields,  $B = 500, 2000,$  and  $6000 \mu\text{G}$ , are shown in comparison with the observed X-ray [16] and radio [35,13] data. At higher frequencies the synchrotron power is always about half the TeV-band  $\gamma$ -ray power on account of the equal likelihood of neutral and charged pions being produced in hadronic collisions. The non-thermal X-ray emission is therefore always contributed by primary electrons.

To be noted from the figure is that for a field strength of 2 mG the radio synchrotron flux is similar to the observed flux, so the primary electrons must be very few because they would contribute only the remaining fraction of the observed radio flux, thus further lowering the  $e/p$  ratio in accelerated particles [15]. This limit is much more severe, if the distance to RX J1713.7-3946 is more than 1 kpc, and the age correspondingly more than 1600 years. It is also more severe, if the effective GeV-to-TeV spectral index of cosmic-ray nucleons in the source is softer,  $\alpha \geq 1.8$ , and

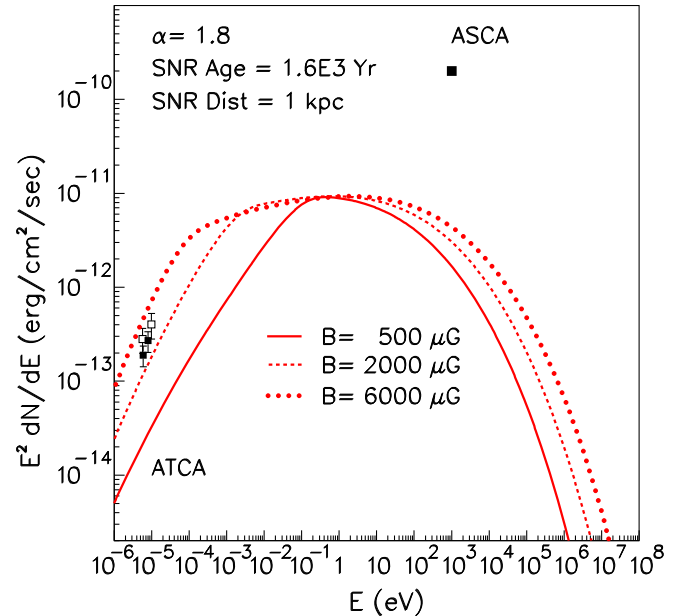


Fig. 1. The synchrotron radiation contributed by secondary electrons produced in RX J1713.7-3946 assuming a source distance of 1 kpc and the SNR age as 1600 years. The cosmic-ray particle spectrum follows (8) and (9) with  $\alpha = 1.8$ . The curves show the synchrotron spectra for magnetic fields  $B = 500, 2000,$  and  $6000 \mu\text{G}$ . The ATCA data (open marks) are based the brightness of the NW rim of RX J1713.7-3946 [35] scaled to the entire remnant with a factor 3 based on the angular distribution of TeV gamma-ray emission [13]. The data points (closed marks) are taken from [13], where they are referenced as private communication. See text for discussions.

it is relaxed in the opposite case. One should note that in mG-fields GHz-band synchrotron emission is emitted by electrons with about 300 MeV kinetic energy, i.e. below the relativistic transition. The effective spectral index must be measured by comparing the 1 GeV flux and the  $\sim 10$  TeV flux of cosmic-ray nucleons, which is considerably softer than the local spectral index near 1 TeV. Measurements of the radio synchrotron of a large number of shell-type SNRs indicate that in the GeV band, the spectral index is locally around 2 [36], whereas at 1–10 TeV the local spectral index should be closer to 1.5 [32], so on average we may expect  $\alpha \simeq 1.8$ . Consequently, a multi-mG magnetic field is unlikely to exist in a large fraction of the synchrotron emission region or  $\alpha$  must be significantly smaller than 1.8 (i.e., the spectrum is harder). This result is conservative, because we are ignoring secondary electrons that were produced in the first half of the time since the SN explosion.

The recent observation of rapid variability of X-rays of RX J1713.7-3946 [18] has been interpreted as evidence for the notion that the magnetic field of the hot spots (two compact regions) could be as large as mG level. These compact regions are in only a few arcseconds and likely present transient acceleration sites of high-energy electrons. Our calculations shows that, if such strong magnetic field exists in SNR shell, they are unlikely to fill the entire remnants.

Table 1 summarizes the limits on the averaged magnetic field strength for various values of the effective GeV-to-TeV spectral index of cosmic-ray nucleons and different values for the age of RX J1713.7-3946. The contribution of synchrotron radiation by secondary electrons is compared with the integrated flux density 20 Jy at 1.4 GHz, which is the result of [35] for the NW region but scaled to the entire remnant with a factor 3 based on the angular distribution of TeV gamma-ray emission [13]. This scaling factor carries a sizable uncertainty not less than 30%, largely owing to systematic uncertainty in the background subtraction in the radio data. Some similar works [13,8,35] have used a scaling factor of 2 for the entire remnant.

#### 4.2. Neutrinos

High-energy cosmic neutrinos are inevitably produced in parallel with hadronic  $\gamma$ -rays. Therefore, TeV-band  $\gamma$ -ray sources represent the prime targets to search for cosmological neutrinos. Several calculations on the expected  $\gamma$ -ray and neutrino spectra were made for parametrized spectra of hadronic particles in the energy range of neutrino detectors,  $E \approx (1-1000)$  TeV [20–26], usually by assuming a simple power-law proton spectrum or a power-law with an exponential cut-off. In contrast, our neutrino production matrix can be applied to cosmic-ray nucleon spectra of any form. Also, the particle yields in the parameterizations can be underestimated because they are often based only on the pion channels. Our production matrix accounts for all relevant decay processes in cosmic-ray hadronic interactions. As shown in Fig. 2, we find that using the same cosmic-ray spectrum, our production matrix gives about 15–20% more  $\gamma$ -rays at all energies. Our production matrix also yields an approximately 30% more muon neutrinos than the parametric model [25] after full mixing. The excess of  $\gamma$ -rays and neutrinos in this figure agrees with the conclusion of our earlier study [1], which has considered the full picture of  $\gamma$ -ray production in hadronic interactions and indicated about 20% more hadronic  $\gamma$ -rays relative to  $\gamma$ -rays from  $\pi^0$  decays alone. Also note that  $\eta$ -decays contribute about 8–10% and kaons also have roughly the same contribution [1]. Only a few percent of  $\gamma$ -rays are contributed by other decay processes (together with the direct  $\gamma$ -ray production). For a given  $\gamma$ -ray or neutrino flux, our

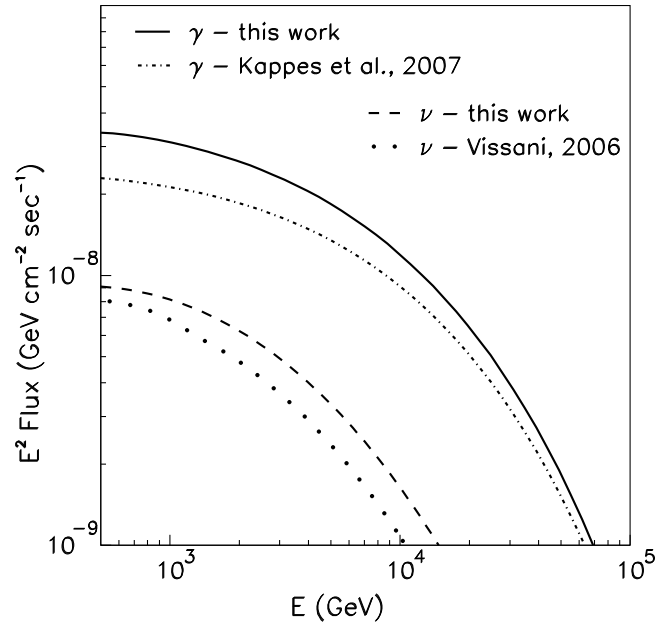


Fig. 2. The  $\gamma$ -ray and raw  $\nu_\mu$  spectra from the cosmic-ray source RX J1713.7-3946 derived using the production matrix discussed in this work, shown in comparison with results of published parametrizations [22,24,25] based on the same cosmic-ray particle spectrum. With the same generating cosmic-ray particle spectrum, our production matrix gives about 15–20% more  $\gamma$ -rays at all energies. Our calculation also shows about 30% more neutrinos than the parametric model of Kappes et al. [25] after considering all relevant decay processes in the cosmic-ray hadronic interactions. The calculations on  $\nu_\mu$  spectra indicate that the parametric model of Vissani [22] gives an overall lower raw  $\nu_\mu$  yield for the same  $\gamma$ -ray flux before taking neutrino oscillations into account.

production matrix therefore implies a lower flux of cosmic-ray nucleons than estimated using the parametric models [24,25].

In high-energy hadronic interactions, the resulting initial  $\nu$  flavor ratio from  $\pi$  decays is  $\nu_e : \nu_\mu : \nu_\tau = 1 : 2 : 0$ . However, the neutrino oscillations transform this ratio to 1:1:1, i.e., full mixing, because the SNR size of  $\sim 10$  pc implies a substantial range of neutrino path lengths, wider than the neutrino oscillation wavelength  $L_{\text{OSC}} = (4\pi E/\Delta m^2)\hbar c \simeq 0.8(E/\text{TeV})(\Delta m^2/10^{-10} \text{ eV}^2)^{-1} \text{ pc}$  [37]. Therefore, it is reasonable to expect the  $\nu_\mu$  spectrum arriving at Earth to be about 1/3 of the total  $dN_\nu/dE$ . The resulting  $\nu_\mu$  spectrum is only weakly dependent of the relative fraction of  $\nu_e$ 's and  $\nu_\mu$ 's at the source. Other studies [21,22] have calculated high-energy neutrinos from galactic sources considering the

Table 1  
Relative contribution of synchrotron radiation by secondary electrons in RX J1713.7-3946 to the observed radio flux in different source models and magnetic fields near the SNR shell

Index	Age (Yr)	B ( $\mu\text{G}$ )	Ratio (%)	B ( $\mu\text{G}$ )	Ratio (%)	B ( $\mu\text{G}$ )	Ratio (%)	B ( $\mu\text{G}$ )	Ratio (%)
$\alpha = 1.6$	1600	500	3.4	1000	8	2000	17	4000	40
$\alpha = 1.8$	1600	500	8	1000	18	2000	41	4000	95
$\alpha = 1.8$	10,000	500	48	1000	111	2000	255	4000	594
$\alpha = 2.0$	1600	500	21	1000	50	2000	119	4000	279

The relative contribution of synchrotron radiation in this table are calculated relative to the radio data of integrated flux density 20 Jy at 1.4 GHz, which is the result of [35] scaled to the entire remnant with a factor 3 based on the angular distribution of TeV gamma-ray emission [13].

actual neutrino mixing angles for point sources. For a comparison of the neutrino source functions by our production matrix and the parametric model [22], we therefore must consider the  $\nu_\mu$  spectra from the TeV  $\gamma$ -ray source RX J1713.7-3946 before neutrino oscillations. In Fig. 2, the  $\nu_\mu$  spectrum is calculated using the production matrix and a generating cosmic-ray particle spectrum [1] that is determined as best-fitting the observed HESS  $\gamma$ -ray data of RX J1713.7-3946; the  $\nu_\mu$  spectrum by the parametric model [22] is calculated based on the same  $\gamma$ -ray spectrum. As seen in this figure, the parametric model gives overall lower raw  $\nu_\mu$  yield from RX J1713.7-3946.

Practically, neutrinos and anti-neutrinos are not distinguishable in neutrino telescopes. Therefore, full neutrino mixing is usually assumed for the  $\nu$  spectrum. Fig. 3 shows the  $\nu_\mu$ -induced muons which may be detected in an IceCube-like experiment [26] from TeV  $\gamma$ -rays sources such as RX J1713.7-3649 [13], MGRO J2019+37 [26] and Vela Jr. [38], together with the background from atmospheric neutrinos. The  $\nu_\mu$ -induced muons for each source example and the atmospheric background are calculated by a parametric model [39], including the neutrino attenuation due to scatterings within the Earth.

In calculating the  $\nu_\mu$ -induced muon event rate, the generating cosmic-ray particle spectrum for each source was obtained by fitting the observed  $\gamma$ -ray spectra using our gamma-ray production matrix [1], from which the  $\nu$ -spec-

tra are determined using the neutrino production matrix (5) and assuming full mixing. Note that a TeV  $\gamma$ -ray spectrum from MGRO J2019+37 is not available at this time. Therefore a fit was performed using EGRET data for 3EG J2021+3716 [26]. A more reliable calculation will depend on a measurement of the TeV  $\gamma$ -ray spectrum of this source.

The charged-current and neutral-current cross sections, the inelasticity involved in  $\nu N \rightarrow \mu^\pm + X$  interactions, and the range of the muons in the detector are based on the theoretical results of [39–41]. The  $\nu$ -induced muon event rate for the atmospheric background is then calculated using the parametrized atmospheric neutrino background as derived in [42], both vertically and horizontally, and assuming an angular resolution element of  $3 \text{ deg}^2$  (1 deg uncertainty radius), which roughly corresponds to the angular resolution of IceCube. As seen in Fig. 3, the calculations indicate a good detectability of high-energy neutrinos from the high-energy  $\gamma$ -ray sources at a few TeV in muon energy, or about 10 TeV neutrino energy. An accumulation of data over about 5–10 years would allow testing the hadronic origin of TeV  $\gamma$ -rays.

The lepton and neutrino production matrices are applicable for arbitrary cosmic-ray hadron spectra. The main systematic uncertainty is that of the simulation tool DPMJET itself. DPMJET has been extensively tested against data for accelerator experiments [1,2,43], for the simulation of cosmic-ray air shower problems [44,45], and for the atmospheric  $\gamma$ -ray and neutrino production [46]. Although the uncertainty for hadronic productions simulated by DPMJET differs with simulation energy as well as the interaction products, it is as good as at least within 15% [43,45].

## 5. Conclusion

In addition to Galactic  $\gamma$ -ray emission, the Galactic neutrino emission could provide complementary information on the existence of hadronic processes in astrophysical objects and also on the origin of Galactic cosmic rays. Here we have calculated the  $e^\pm$ ,  $\nu_e$  and  $\nu_\mu$  production in cosmic-ray interactions and derived matrices that allow to estimate the spectra of secondary leptons for arbitrary spectra of the parent hadronic cosmic rays.

With the production matrices, we calculate the synchrotron radiation of secondary electrons in the shell-type SNR RX J1713.7-3649 under the assumption that the observed TeV-scale gamma-ray emission is hadronic in origin. We find that the radio synchrotron flux of the secondary electrons exceeds the observed flux level if the magnetic field strength is too high. The multi-mG fields recently invoked to explain the X-ray flux variations [18] are therefore unlikely to extend over a large fraction of the radio-emitting region or the spectrum of hadronic cosmic rays in the 0.1–100 GeV energy window must be unusually hard.

Our calculations for neutrinos show that the neutrino detection rates from the TeV  $\gamma$ -ray sources RX J1713.7-3946 and Vela Jr. are promising for muon energies of a

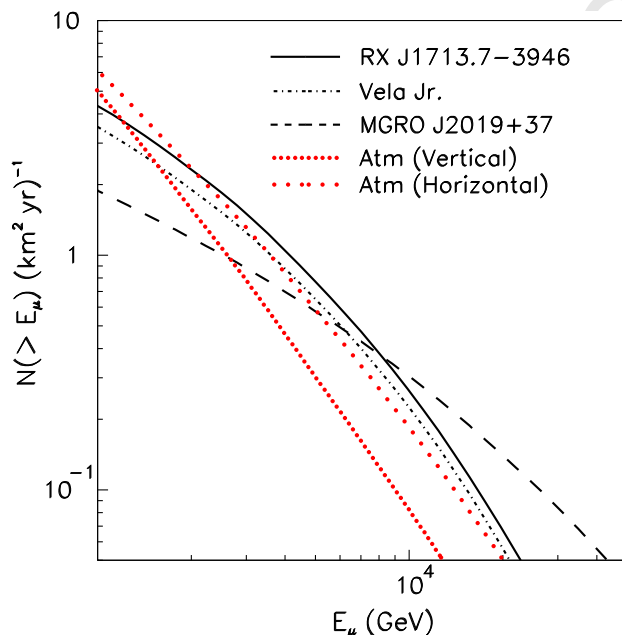


Fig. 3. Integrated fully mixed ( $\nu_\mu + \bar{\nu}_\mu$ )-induced muon rates from the TeV  $\gamma$ -ray sources RX J1713.7-3946 (solid line), Vela Jr. (dash-dot line) and MGRO J2019+37 (dash line) above a given muon energy within an IceCube-like detector. The generating cosmic-ray spectra are obtained by fitting the observed TeV  $\gamma$ -rays of RX J1713.7-3946 [13], Vela Jr. [38], and MGRO J2019+37 [39], using the production matrices for gamma-rays and neutrinos. The atmospheric background rates, vertical (long dot) and horizontal (short dot), are calculated using the parametrization of [42] and assuming an angular resolution element of  $3 \text{ deg}^2$ .

549 few TeV, or in other words, about 10 TeV neutrino energy.  
550 An accumulation of data over about 5–10 years would  
551 allow testing the hadronic origin of TeV  $\gamma$ -rays.

552 The production matrices for  $e^-$ ,  $e^+$ ,  $\nu_e$ ,  $\bar{\nu}_e$ ,  $\nu_\mu$  and  $\bar{\nu}_\mu$  will  
553 be made available for download at [http://cherenkov.physics-](http://cherenkov.physics.iastate.edu/lepton-prod)  
554 [ics.iastate.edu/lepton-prod](http://cherenkov.physics.iastate.edu/lepton-prod).

### 555 Acknowledgements

556 The author C.-Y. Huang would like to thank Y. Liu for  
557 his helpful comments. Support by NASA under award No.  
558 NAG5-13559 is gratefully acknowledged.

### 559 References

560 [1] C.-Y. Huang, S.-E. Park, M. Pohl, C.D. Daniels, *Astropart. Phys.* 27  
561 (2007) 429.  
562 [2] S. Roesler, R. Engel, J. Ranft, *Advanced Monte Carlo for Radiation*  
563 *Physics, Particle Transport Simulation and Applications (MC 2000)*,  
564 Lisbon, 2000.  
565 [3] Steve R. Blattinig, Sudha R. Swaminathan, Adam T. Kruger, Moussa  
566 Ngom, John W. Norbury, *Phys. Rev. D* 62 (2000) 094030.  
567 [4] T. Kamae, N. Karlsson, M. Tsunefumi, A. Toshinori, K. Tatsumi,  
568 *Astrophys. J.* 647 (2006) 692.  
569 [5] K. Koyama, R. Petry, E.V. Gotthelf, et al., *Nature* 378 (1995) 255.  
570 [6] K. Koyama, K. Kinugasa, K. Matsuzaki, et al., *PASJ* 49 (1997) L7.  
571 [7] J.W. Keohane, R. Petry, E.V. Gotthelf, et al., *Astrophys. J.* 484  
572 (1997) 350.  
573 [8] P. Slane, B.M. Gaensler, T.M. Dae, et al., *Astrophys. J.* 525 (1999)  
574 357.  
575 [9] G.E. Allen, J.W. Keohane, E.V. Gotthelf, et al., *Astrophys. J.* 487  
576 (1997) L97.  
577 [10] K.J. Borkowski, J. Rho, S.P. Reynolds, K.K. Dyer, *Astrophys. J.* 550  
578 (2001) 334.  
579 [11] M. Pohl, *Astron. Astrophys.* 307 (1996) L57.  
580 [12] F.A. The HESS Collaboration, Aharonian, et al., *Astron. Astrophys.*  
581 437 (2005) L7.  
582 [13] The HESS Collaboration, F.A. Aharonian, et al., *Astron. Astrophys.*  
583 449 (2006) 223.  
584 [14] O. Reimer, M. Pohl, *Astron. Astrophys.* 390 (2002) L43.  
585 Q1 [15] B. Katz, E. Waxman, *JCAP* arXiv:0706.3485, in press.

[16] J.S. Hiraga, Y. Uchiyama, T. Takahashi, F.A. Aharonian, *Astron.* 586  
*Astrophys.* 431 (2005) 953. 587  
[17] L. O’C. Drury et al., *Space Sci. Rev.* 99 (2001) 329. 588  
[18] Y. Uchiyama, F.A. Aharonian, T. Tanaka, T. Takahashi, Y. Maeda, 589  
*Nature* 449 (2007) 576. 590  
[19] T. Takahashi, et al., *PASJ*, arXiv:0708.2002, in press. 591  
[20] J. Alvarez-Muñiz, F. Halzen, *Astrophys. J.* 576 (2002) L33. 592  
[21] M.L. Costantini, F. Vissani, *Astropart. Phys.* 23 (2005) 477. 593  
[22] F. Vissani, *Astropart. Phys.* 26 (2006) 310. 594  
[23] P. Lipari, *Nucl. Instrum. Methods Phys. Res. A* 567 (2006) 405. 595  
[24] S.R. Kelner, F.A. Aharonian, V.V. Bugayov, *Phys. Rev. D* 74 (2006)  
034018. 596  
[25] A. Kappes, J. Hinton, C. Stegmann, F.A. Aharonian, *Astrophys. J.* 598  
656 (2007) 870. 599  
[26] J.F. Beacom, M.D. Kistler, *Phys. Rev. D* 75 (2007) 083001. 600  
[27] M. Honda, T. Kajita, K. Kasahara, S. Midorikawa, *Phys. Rev. D* 52  
(1995) 4985. 601  
[28] J.H. Scanlon, S.N. Milford, *Astrophys. J.* 141 (1965) 718S. 602  
[29] L.V. Volkova, in: *Erice 1988, Proceedings, Cosmic Gamma Rays,*  
*Neutrinos, and Related Astrophysics.* 603  
[30] S.M. Barr, T.K. Gaisser, P. Lipari, S. Tilav, *Phys. Lett. B* 214 (1988)  
147. 604  
[31] C.-Y. Huang, M. Pohl, in: *Proceedings of 30th International Cosmic*  
*Ray Conference 2007.* 605  
[32] E. Amato, P. Blasi, *Mon. Not. R. Astron. Soc.* 371 (2006) 1251. 606  
[33] E.G. Berezhko, D.C. Ellison, *Astrophys. J.* 526 (1999) 385. 607  
[34] Z.R. Wang, Q.-Y. Qu, Y. Chen, *Astron. Astrophys.* 318 (1997) L59. 608  
[35] J.S. Lazendic, P.O. Slane, B.M. Gaensler, et al., *Astrophys. J.* 602  
(2004) 271. 609  
[36] D.A. Green, *AIP Conf. Proc.* 558 (2001) 59. 610  
[37] R.M. Crocker, F. Melia, R.R. Volkas, *Astrophys. J.* 141 (Suppl.)  
(2002) 147. 611  
[38] The HESS Collaboration, F.A. Aharonian, *Astrophys. J.* 661 (2007)  
236. 612  
[39] M.D. Kistler, J.F. Beacom, *Phys. Rev. D* 74 (2006) 063007. 613  
[40] R. Gandhi, C. Quigg, M.H. Reno, I. Sarcevic, *Astropart. Phys.* 5  
(1996) 81. 614  
[41] R. Gandhi, C. Quigg, M.H. Reno, I. Sarcevic, *Phys. Rev. D* 58 (1998)  
093009. 615  
[42] L.V. Volkova, *Sov. J. Nucl. Phys.* 31 (1980) 784. 616  
[43] J. Ranft, *Phys. Rev. D* 51 (1995) 64. 617  
[44] J. Knapp et al., *Astropart. Phys.* 19 (2003) 77. 618  
[45] T. Antoni et al., *J. Phys. G: Nucl. Part. Phys* 27 (2001) 1785. 619  
[46] K. Kasahara et al., *Phys. Rev. D* 66 (2002) 052004. 620  
621  
622  
623  
624  
625  
626  
627  
628  
629  
630